Cellulose (2021) 28:7123–7142
https://doi.org/10.1007/s10570-021-03917-4

ORIGINAL RESEARCH

Laccase-modified cornstalk pith for cleanup of spilled diesel oil

Dan Peng · Wenjie Li · Liuchun Zheng

Received: 16 October 2020 / Accepted: 4 May 2021 / Published online: 28 May 2021

Abstract Repurposing corn stalk pith (CSP) from agriculture waste is significant for environmental protection and sustainability. In this work, enzymatic modification of inexpensive and biodegradable CSP was used to prepare two environmentally friendly and efficient oil sorbents by a one-step in situ strategy: (1) cellulose-grafted octadecylamine via the laccase (LAC)-2,2,6,6-tetramethylpiperidine-1-oxyl (TEMPO) system (LCSP) and (2) lignin-grafted octadecyl gallate via the LAC-guaiacol system (GCSP). The oil sorbents were characterized, revealing that they had low density, were hydrophobic (water contact angle (CA) up to 129.7°–144.9°), and had a good diesel sorption capacity in the range of 34–41 g/g, superior to those of most agricultural waste materials reported to date. The sorption kinetic results show that LCSP and GCSP fit a pseudo-second-order model. Sorption equilibrium was simulated by four commonly used isotherm models, and error analysis was performed, confirming that the Freundlich equation best fit the experimental data. Oil sorption was exothermic, with the best oil sorption performance achieved at room temperature. The sorption by the two sorbents of simulated low-concentration dispersed oil was similar, and the sorption by GCSP of high-concentration suspended oil was the best. The effects of solution pH, ion species, salinity, and temperature were also investigated. Overall, the obtained materials demonstrated outstanding environmentally friendly characteristics due to their high availability, agricultural origin and potential for use in remediating light oil spills owing to their fast sorption and high and stable sorption capacity.

Keywords Agricultural waste · Lignocellulose · Sorption · Hydrophobicity · Oil spill

Supplementary Information The online version contains supplementary material available at https://doi.org/10.1007/s10570-021-03917-4.

D. Peng (✉) · W. Li
Department of Transportation and Environment, Shenzhen Institute of Information Technology, Shenzhen 518172, People's Republic of China
e-mail: pengdan987@hotmail.com

W. Li
School of Earth and Environment, Anhui University of Science & Technology, Huainan 232001, People's Republic of China

L. Zheng (✉)
School of Environment, Guangzhou Higher Education Mega Center, South China Normal University, Guangzhou 510006, People's Republic of China
e-mail: lczhengscnu1@163.com

Introduction

Water pollution caused by oil leakage during oil exploitation, transportation, storage, and utilization

has a serious adverse effect on the surrounding environment and human health and has attracted a great deal of attention (Doshi et al. 2018). In response to such environmental disasters, a variety of methods have been developed to treat oily wastewater, including in situ combustion, mechanical separation (booms, skims, etc.), air flotation, chemical methods (surfactants and dispersants), electrochemical treatment and bioremediation (microorganisms and biological agents) (Moosai and Dawe 2003; Navarathna et al. 2020; Prendergast and Gschwend 2014; Yang et al. 2009). However, these treatments have many limitations based on the environmental conditions: for example, in situ combustion is suitable only for low wind speed conditions and generates air pollutants. Dispersants quickly reduce the water/oil interfacial tension and break the oil into smaller droplets, which are mixed into the water system and diffuse throughout the surface water (Ibrahim et al. 2010; Wu et al. 2017). Biological methods have no secondary pollution, but their low economic benefits, slow rates, and rigorous conditions are nonnegligible disadvantages (Yang et al. 2019). Therefore, as a recyclable, efficient, and convenient method, sorption is frequently used to separate oil–water mixtures (Demirel Bayık and Altın 2018). Different forms of sorption materials, such as biochar (Navarathna et al. 2020), polypropylene webs (Thilagavathi et al. 2018), foams (Chen et al. 2019) and sponges (Li et al. 2019; Zhou et al. 2019), have been developed to tackle emergencies (Zhang et al. 2018). However, these functional materials are normally difficult to degrade, which can cause secondary environmental pollution. Therefore, it is urgent to develop novel renewable and efficient sorbent materials for oil/water separation. Using agricultural byproducts or wastes to produce sorbents with high surface hydrophobicity and sorption capacity may be a good choice owing to their high quantity, low cost, and biodegradability (Navarathna et al. 2020). Corn stalk (CS) is a major agricultural waste, with a production of approximately 250 million tons per year in China (Chen et al. 2008), and has been developed as a sorbent to remove various inorganic (Guo et al. 2015; Vafakhah et al. 2014; Zhang et al. 2018) and organic (Ge et al. 2016; Lamichhane et al. 2016; Tran et al. 2015) pollutants from water/wastewater. However, the selective oil sorption capacity of raw corn stalk (RCS) is limited due to the large number of polar functional groups, especially surface hydroxyl groups, in its structure. Therefore, the raw materials must be modified to optimize their surface characteristics for better performance.

At present, physical and chemical methods are commonly used for biomass modification. Sidiras et al. fabricated an oil sorbent made of wheat straw using automatic hydrolysis, and the prepared sorbent can adsorb diesel at 6.65 g/g (Sidiras et al. 2014). This modification method is easy to operate, but the sorption effect of the product is not ideal. Li et al. investigated the acetylation of cellulose fibers extracted with acidified sodium chlorite and sodium hydroxide from corn straw and observed an increase in the sorption capacity for pure diesel from 24.38 g/g to 52.65 g/g. However, the production process is complicated, produces too much acid wastewater and is time consuming (Li et al. 2013). Some monomer grafting methods require suitable initiators, such as cerium ammonium nitrate (CAN), various persulfates, azobisisobutyronitrile (AIBN), and Fenton reagent ($Fe(II)$-H_2O_2) (Hokkanen et al. 2016), which necessitates the use of many toxic and environmentally harmful reagents. Considering energy savings, economic benefits, and environmental friendliness, some researchers have begun to investigate possible biotechnology methods based on the use of enzymes (Skals et al. 2007). In our previous studies, cellulase was utilized for the modification of CS, leading to a diesel sorption rate 3 times greater than that of RCS (Peng et al. 2013, 2018), but the hydrophobicity of the material was still poor. Zhang et al. reported a facile one-step method to modify the surface of polyvinylidene fluoride with dopamine using tyrosinase as a catalyst, and the resultant membrane exhibited superoleophobicity and oil repellency (Zhang et al. 2019).

Using functional enzymes to improve surface hydrophobicity is rare and still a challenge (Younis et al. 2016). In this work, laccase (LAC) was selected to improve the hydrophobicity of the investigated biomass because LAC not only is eco-friendly (using air and producing water as the only byproduct) but also works under mild, energy-saving conditions (Kudanga et al. 2011). Conventionally, fungal LACs are mainly responsible for lignin removal and modification, but studies have shown that LAC cannot directly oxidize rigid structures such as lipophilic extracts, which must be combined with synthetic or natural low-molecular-weight phenolic compounds (mediators). The LAC-mediator system (LMS) can expand the oxidation

ability of LAC, and LMS applications have made progress in the food industry, textile industry, pharmaceutical industry, etc., especially in the paper industry, such as in delignification (Garcia-Ubasart et al. 2012), pulp bleaching (Fillat and Roncero 2010; Moldes and Vidal 2011), and increases in wet strength (Aracri et al. 2011). The most efficient LAC mediators are 2,2-azino-bis(3-ethylbenzothiazoline-6-sulfonic acid) (ABTS), 1-hydroxybenzotriazole (HBT), vanillin, and ferulic acid and guaiacol (Singh and Arya 2019). These small mediators can penetrate the fiber wall structure to solve steric hindrance (Filgueira et al. 2017). Long-chain hydrophobic compounds can be grafted onto the lignin surface to increase the hydrophobicity of the material (Kudanga et al. 2010). Recently, many studies have reported that carboxylate and aldehyde functional groups can be introduced into solid native cellulose under aqueous and mild conditions by LAC/2,2,6,6-tetramethylpiperidine-1-oxyl (TEMPO)-mediated oxidation, which operates in milder conditions than TEMPO/NaBr/NaClO treatment, generating less environmentally harmful residues (Lavoine et al. 2012). Aldehyde functional groups can react with the amino group of octadecylamine by a Schiff-base reaction, which can increase the hydrophobicity of cellulose (Aracri et al. 2011). This modification should make cellulose a better oil sorbent and might help it float to stay in contact with surface oil. However, there are no previous reports related to the functionalization of lignocellulosic materials to produce oil sorbents. Based on these principles, LAC-based chemoenzymatic grafting of hydrophobic organic compounds has the potential to be a viable way to produce efficient and biodegradable oil sorbents (Kudanga et al. 2010).

CS is composed of three parts: leaf, rind, and pith. These three parts have significant differences in lignocellulose content, material structure, and properties. The cellulose content of corn stalk pith (CSP) can reach 40.5%, and the lignin content is 6.72%. In particular, CSP has a sponge-like structure with a low density of abundant natural pores, which shows that CSP is suitable for the preparation of sorbents. However, in most studies, only whole CS has been the focus of development. In this study, CSP was used as the raw material for oxidation with LAC/mediators under mild conditions to develop an oil sorbent with good hydrophobic properties. Two different LMS systems were used to catalyze the grafting of the same length of alkyl chains, but the difference lies in the effects on cellulose and lignin. No previous work has simultaneously investigated the behavior of different types of oil sorption onto a stalk-based material modified with two routes of LMS. The two modification processes used are shown in Fig. 1a. LCSP is prepared by selectively oxidizing primary hydroxyl groups in straw fibers to aldehyde groups through the laccase-TEMPO mediator system, and then it continues to react with the amine groups of octadecylamine and graft functional molecules through -C = N- bonds. GCSP uses low-molecular-weight phenolic compounds to generate resonance-stabilized phenoxy radicals under the enzymatic oxidation reaction of laccase, and then it couples with free radicals in octadecyl esters through -O- to complete the hydrophobic long-chain alkyl connection. This process is depicted in Fig. 1b. The sorption capacity of the two sorbents was compared in the removal of low-concentration suspended oil and high-concentration floating oil from water. The effects of solution pH, temperature, ion species and concentration on suspended oil removal were investigated. The sorption mechanism was also studied through characterizing the physical–chemical properties of the materials and establishing kinetic, isothermic, and thermodynamic models.

Material and methods

Materials

The CS used in this study originated from Baise, Guangxi Province, China. The raw material was washed and dried at room temperature. CSP was manually separated from CS and ground in a grinding machine (Retsch RM 100, China). The fraction with a particle size between 20 and 40 mesh was pretreated with hot water for 60 min, washed with distilled water, and dried at 60 °C for 24 h. Cellulose and lignin on the CSP surface were exposed after pretreatment for later modification.

LAC from *Trametes versicolor* and TEMPO were supplied by Sigma-Aldrich (USA). The hydrophobic

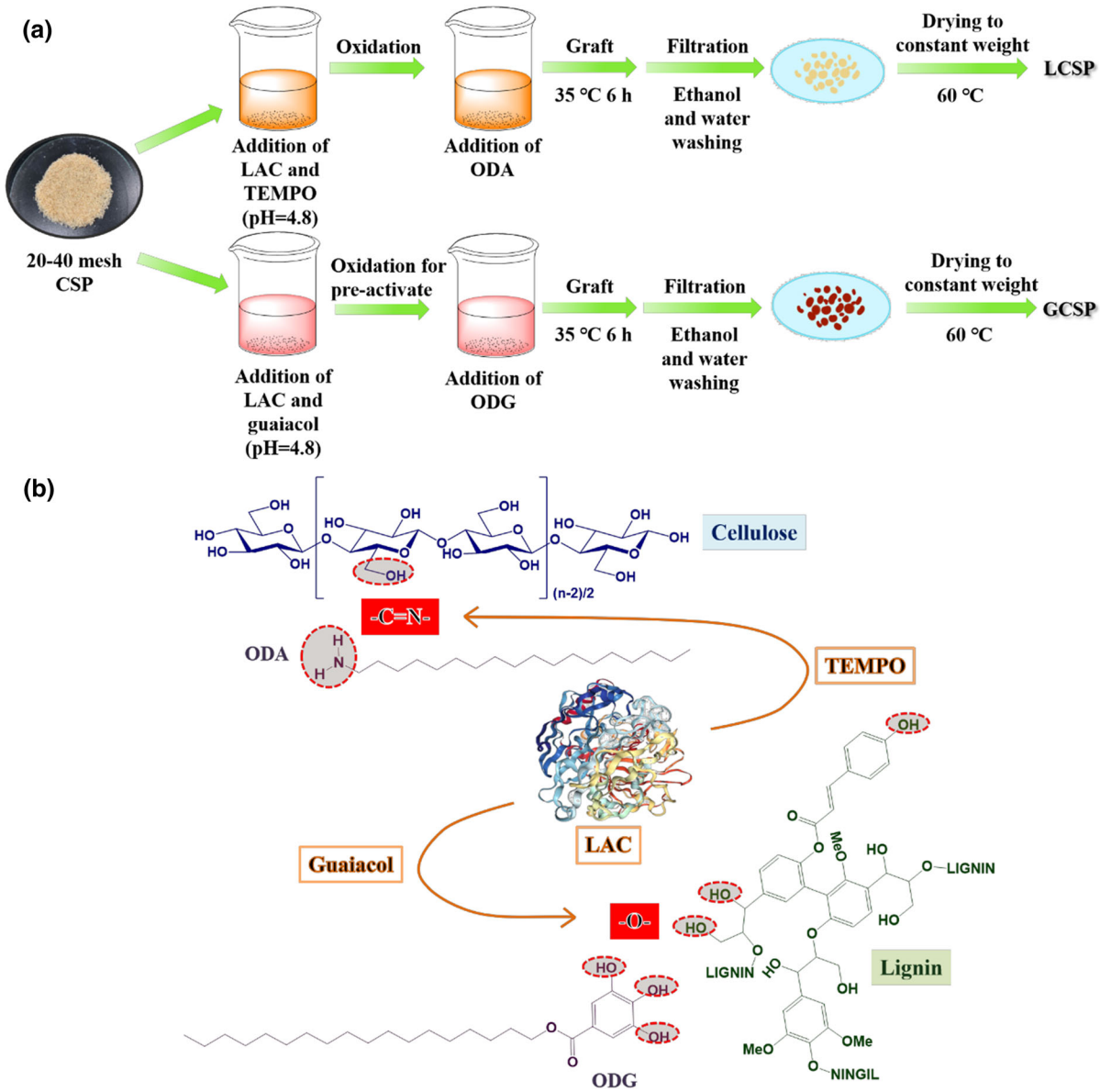

Fig. 1 **a** Preparation schematic of LCSP and GCSP. **b** Modification mechanisms

compounds octadecylamine (ODA) and octadecyl gallate (ODG) and guaiacol were supplied by Aladdin (Shanghai, China). The diesel oil used as the experimental oil was collected from a local service station and had a density of 0.839 g/cm^3 and a viscosity of 6.50 cP at 20 °C, classifying it into the category of light petroleum derivates rather than crude oils, which suggests that it may be difficult to trap and adsorb this light oil in sorbent systems. Milli-Q water (18.2 MΩ cm) was used throughout the experiments.

LAC modification of CSP

LAC-catalyzed biografted cellulose-based materials were synthesized as described in our previous studies. First, 2% CSP (w/w) was oxidized with 4.99 mM TEMPO and 100 U/g LAC in sodium acetate buffer (pH 4.8), and then 8.91 mM ODA was grafted for 6 h. Once the reaction was completed, the reaction mixture was heated at 90 °C for 15 min to inactivate LAC, and the resulting modified CSP was collected and

ultrasonically washed with ethanol and pure water to remove excess chemicals. Then, the CSP biografted with ODA was dried to constant weight and stored for the following experiment; this material was denoted as LCSP.

GCSP was prepared using a similar approach. CSP grafted with ODG was obtained by mixing LAC (100 U/g), guaiacol (0.02 M), ODG (5 mM) and 2% CSP by weight (w/w) in 50 mM sodium acetate buffer (pH 4.8) for 6 h. The resulting material, denoted as GCSP, was filtered, repeatedly ultrasonically washed with ethanol, washed with distilled water, and dried at 60 °C for 24 h. Both sorbents were stored in zip-lock bags until further use.

Characterization methods

CSP, LCSP and GCSP were individually characterized by scanning electron microscopy (SEM, ZEISS GeminiSEM 300, Germany) at 5 kV. The obtained SEM images were used to compare the morphology and microstructure of the materials. The Brunauer–Emmett–Teller (BET, ASAP 2020, Micromeritics, USA) method was used to calculate the specific surface area by obtaining nitrogen adsorption isotherms at 77 K, and the pore volume and average pore diameter were determined by the Barret-Joyner-Halenda (BJH) method. The C, H, O, and N elemental contents of the samples were measured using an element analyzer (EA, Vario EL Cube, Elementar, Germany). The crystal structures of the sorbents were determined by X-ray diffractometry (XRD, D8 ADVANCE, Bruker, Germany) using a Cu Kα target (X-ray λ = 1.54 Å). The XRD analysis was carried out in a 2θ range of 5°–60° with a goniometer speed of 4°/min. Fourier transform infrared spectroscopy (FTIR) was carried out to characterize surface functional groups and chemical bonds in the range of 4000–400 cm^{-1} with 4.0 cm^{-1} resolution and 64 scans for each data point using an FTIR spectrometer (Vetex70, Bruker, Germany). X-ray photoelectron spectroscopy (XPS) measurements were performed using a Thermo Fisher ESCALAB XI+(UK) system with Al Kα radiation, and the binding energy was calculated relative to the survey spectra at 200 eV and the C1s spectra at 284.8 eV with an accuracy of ± 0.05 eV.

The contact angles (CAs) of liquid (water and oil) drops on the surface of CSP and modified CSP were measured by a dynamic CA goniometer (OCA15EC, DataPhysics, Germany). Briefly, double-sided tape was fixed on a glass sheet, and then the samples were adhered to obtain uniform coverage on the surface of the tape. After placing 10 μL of water or diesel droplets on the surface of the attached sample, an image was collected using the analyzer. The CA values were automatically calculated by the circle fitting method. Each sample was measured at least three times.

Batch sorption experiments

Artificial oil spills were simulated by adding 25 mL of distilled water and 0.125 g of diesel oil to a 50 mL glass beaker at 25 °C and using ultrasonic technology to reduce the surface tension between water and oil to obtain a water/oil mixture (Davoodi et al. 2019). Batch sorption experiments were carried out by conventional methods. Each sorbent was preweighed (approximately 0.01 g), scattered over the surface of the oil/water mixture, allowed to equilibrate for 1 h (150 rpm rotation), and then collected by filtering through a screen. Hexane was used as the extractant after the process reached equilibrium, and the concentration of diesel oil was measured at 225 nm in a UV–visible spectrophotometer (UV-2600, Shimadzu, Japan). The sorption capacity (q_e) and removal efficiency ($\%R$) were calculated by the following expressions:

$$q_e = \frac{(C_0 - C_e)V}{W} \quad (1)$$

$$\%R = \frac{C_e - C_0}{C_0} \times 100\% \quad (2)$$

where C_0 and C_e are the solution concentrations at the initial time and at equilibrium (g/L), respectively; V (L) is the volume of the oil–water mixture; and W (g) is the weight of the sorbent. Sorption measurements were carried out in triplicate for each type of sample to obtain average and standard deviation values.

The variables that may affect sorption capacity and removal efficiency were studied. To determine the effect of pH on oil sorption, the pH of the water added to the beakers was varied (2, 4, 6, 8, 10, and 12) using either 1 M HCl or NaOH with a dosage of 0.4 g/L, an initial diesel concentration of 5000 ppm and a contact time of 1 h. Salt ions (0.1 M HPO_4^{2-}, CO_3^{2-}, SO_4^{2-},

and Cl^-) and sodium chloride at 0–0.2 M were applied to study the effect of salt ion types and salinity on the removal efficiency and sorption capacity. The influence of temperature during sorption was studied using 0.01 g of each sorbent (0.4 g/L) under the abovementioned optimized conditions at water temperatures of 5, 15, 25, 35, and 45 °C.

The sorption kinetics for LCSP and GCSP were determined by immersing the samples for varying contact times from 0 to 90 min in an emulsion with an oil concentration of 5000 ppm. After the designated contact time, the samples were raised and allowed to drip until the equilibrium point. All sorption values were calculated using Eq. (1), and the kinetic curve of sorption (g/g) versus contact time was prepared. The initial oil concentration of the mixture (500–9000 ppm) was varied to collect isotherm data for model fitting while holding other factors constant with 60 min of contact time. All tests were performed in triplicate.

The sorption of high-concentration oil slicks (floating oil) was also studied. The sorbent was put into a clean screen with a known weight and then suspended in an oil–water system with a certain thickness of oil slick. After sorption, the screen was lifted for 3 min and weighed. The sorption capacity (q_e) was calculated by the following expression:

$$q_e = \frac{W_e - W}{W} \quad (3)$$

where W and W_e (g) are the weights of the material before and after sorption, respectively.

Results and discussion

Characterization

Surface morphology

SEM images were taken to observe the surface morphological changes in LCSP and GCSP relative to the surface morphology of CSP. The SEM micrographs displayed the original structure and the regular smooth surface of CSP (Fig. 2a and d). After LAC modification, the materials appeared loose and uneven in structure due to LAC catalytic oxidation and biomodification with ODA or ODG, and this topography may contribute to the high sorption characteristics of the materials. Figure 2e and c show surface and cross-section images of the treated CSP, indicating a tubular structure with holes and voids, which provide appropriate binding sites for diesel. At a magnification of 1000 × (Fig. 2f), attachments can be observed on the surface of GCSP, which can be inferred to be grafted octadecyl ester, which is the reason for the improved hydrophobicity of the material.

Surface area and elemental analysis

The standard BET technique was utilized to assess the effect of grafting on surface area. The obtained surface area, total pore volume, and average pore diameter of the three materials are shown in Table 1.

When grafting ODA or ODG onto CSP, the long alkyl chains caused CSP surface coverage and partial pore blockage, resulting in a decrease from the original CSP surface area (from 3.799 to 2.7244–2.8339 m^2/g). LCSP exhibited a higher total pore volume and average pore size than CSP, which can be attributed to the formation of a greater number of mesopores (2 nm to 50 nm) during modification. This greater number of mesopores was important for the internal propagation and circulation of compounds, and pollutants were more likely to enter and attach to the interior of the adsorbent. The modified ODG coating obtained with the LAC-guaiacol system also reduced the measured GCSP pore volume to 0.003058 cm^3/g, and the average pore diameter increased slightly. This result is consistent with previous explanations that many pores cannot be contacted by water and filled with air. Therefore, like water, the test gas was prohibited from entering most of the surface pores and the larger internal void volume after ODG treatment. Nevertheless, a large amount of oil absorption occurred because the oil directly attached to the nonpolar alkyl chains of ODG, occupying and filling the cracks and depressions on the surface (Navarathna et al. 2020). This process also showed that LMS modification has a greater influence on the structure of cellulose than on that of lignin.

The combustion analysis of elements for the modified sorbents (Table 1) intuitively revealed that the increased C wt% and C/H (∼ 7.9–8.4) weight ratio came from the added long alkyl chains. The lower H wt% values in LCSP and GCSP than CSP resulted from the formation of -C = N- and -O-,

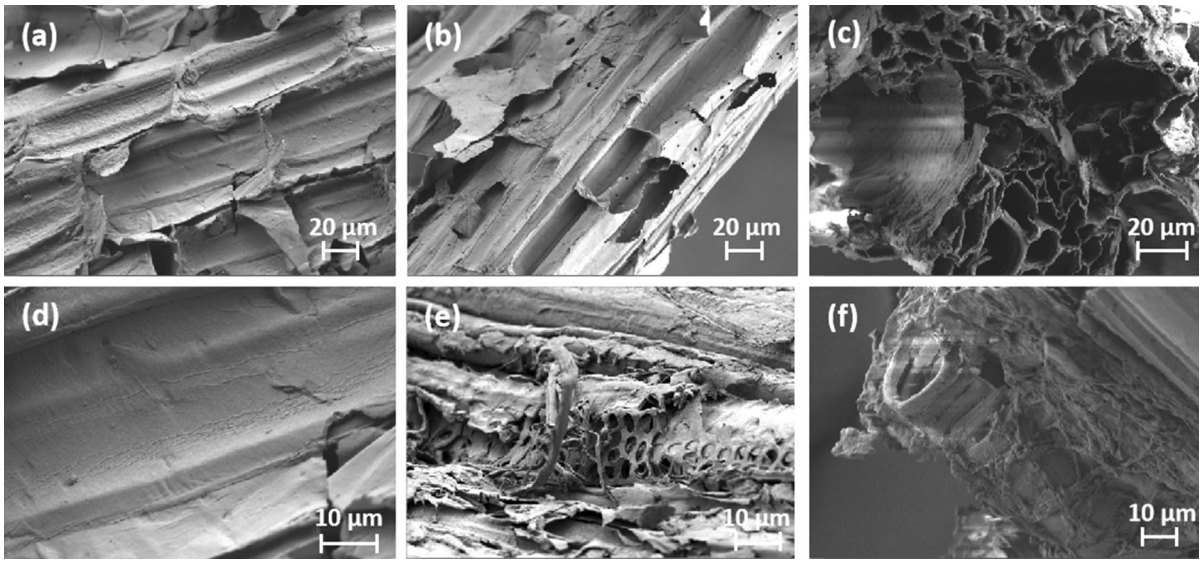

Fig. 2 SEM images of **a**, **d** CSP **b**, **e** LCSP **c**, **f** GCSP

Table 1 Porosity characteristics and elemental analysis of CSP, LCSP, and GCSP

Sample	BET surface area (m^2/g)	Total pore volume (cm^3/g)	Average pore diameter (nm)	C(wt%)	H(wt%)	N(wt%)	O(wt%)
CSP	3.7999	0.003829	4.031	44.23	6.128	0.33	49.312
LCSP	2.7244	0.020720	30.42	44.51	5.63	0.9	48.96
GCSP	2.8339	0.003052	4.307	44.96	5.34	0.52	49.18

respectively, during the grafting reaction. The increase in N wt% in LCSP confirmed the success of ODA grafting. The slightly higher O wt% of GCSP than LCSP may have come from the introduction of guaiacol or ODG. The ratio (O+N)/C showed the polar characteristics of a material, and the lower (O+N)/C weight ratios of both LCSP and GCSP illustrated that the modification improved the surface hydrophobicity of raw CSP.

XRD analysis

The XRD patterns of the materials before and after modification are shown in Figure S1. The shapes of the spectra are similar, and the characteristic diffraction peaks are not shifted, indicating that the modification did not significantly change the crystal structure of the material. However, the (002) diffraction peaks show significant broadening and exfoliation after modification, indicating that the substitution of hydroxyl groups by ODA or ODG broke both inter- and intramolecular hydrogen bonds in cellulose and decreased the degree of crystallinity (Shin et al. 2020). The crystallinity index (*CrI*) has been used to explain the structure of cellulose and is one of the most important indicators of physical, chemical, and mechanical properties. The effect of LMS modification on the *CrI* of the material was explored. From Scherrer's equation (Jiang et al. 2015), the average crystallite sizes of CSP, LCSP, and GCSP were found to be 1.85, 2.80 and 2.36 nm, respectively, which was also in line with the SEM results. The crystallite size of the modified materials was considerably larger than the crystallite size of the untreated material, which may be due to the reduction in the content of amorphous components (such as hemicellulose and other noncellulose components) in the material. Structures with a smaller crystal size tend to absorb

more water than structures with larger crystallite size (Indran et al. 2014). The difference in crystal size between the two modified materials lay in the modification sites, which can also explain the different *CrI* values of LCSP and GCSP. The *CrI* of the raw material was 51.17%, and those of LCSP and GCSP were 21.33% and 37.46%, respectively. The *CrI* value of the material decreased, indicating that the pore structure was loosened by modification, which was conducive to the entry of oil molecules into the internal structure and provided more adsorption space, thereby improving the oil absorption performance. This conclusion was the same as that determined from the above BET analysis. LCSP has a lower *CrI* than GCSP, which is explained by the fact that GCSP modification acts on lignin, belonging to the noncrystalline region, and LCSP acts on cellulose, belonging to the crystalline region, which determines *CrI*.

FTIR analysis

The FTIR method was effectively used to identify the functional groups of the modified materials. Figure S2 shows the FTIR spectra of CSP before and after modification, and some characteristic variations in the FTIR spectra of CSP after grafting are apparent.

In the FTIR spectrum of CSP, the wide and bold adsorption peak at 3340 cm^{-1} was assigned to the -OH stretching vibration of phenols, carboxylic acids, and alcohols, which are widely present in lignocellulosic materials, especially in cellulose, which is a hydrophilic compound, so the intensity of this peak may also indicate the hydrophilicity level of such a material (Oliveira et al. 2020). The spectra of LCSP and GCSP show a significant decrease in the intensity of peaks in the -OH region, which can be attributed to the participation of -OH groups in cellulose in the crosslinking reaction with the functional molecules and is additional proof of the successful hydrophobization of CSP. The peak at approximately 2922 cm^{-1} was assigned to the stretching vibrations of C-H bonds in methyl groups. In the case of LCSP (Figure S2a), in addition to the peaks associated with raw CSP, peaks were observed at 2857 cm^{-1} due to the presence of sp^3 C-H stretching of -CH_2, which confirms the incorporation of the long aliphatic acid chain from ODA into the material during modification. This observation agrees directly with the formation of surface stearamine complexes (Fig. 1b) during LCSP synthesis. The peak at 1728 cm^{-1} was due to the stretching vibration of hydrophobic carbonylic groups (-C = O-), whose intensity became stronger after surface functionalization, implying the successful grafting of ODA or ODG through the oxidation of CSP (Oliveira et al. 2020; Schneider et al. 2019). From the presence of C-H (saturated), CH_2, CH_3, C = C, and C = O groups, it can be inferred that the material had high hydrophobicity and oleophilicity due to the nonpolar chemical affinity of oil with these components (Schneider et al. 2019; Zhang et al. 2020). The strong peaks at 1632, 1604, 1422, 1244, and 1036 cm^{-1} in the CSP spectrum were associated with absorbed O–H stretching, aromatic skeletal vibrations plus C-O stretching, aromatic skeletal vibrations, C-O stretching vibrations, and C-O stretching in C–O–C linkages, respectively, and the intensities clearly decreased after modification. The peak at 1036 cm^{-1} of GCSP was smaller than that of LCSP, which is most likely due to the correlation between the condensation of hydroxyl groups and ether bonds. The three characteristic absorption peaks of cellulose and hemicellulose were at 1156, 1107, and 1036 cm^{-1}, respectively, which were attributed to the absorption of C-O-C in α-glycosidic bonds, C-O absorption, C-C stretching, and C-O stretching (Kacurakova et al. 1998). Compared with the results for CSP, the three bands in the modified samples gradually weakened, indicating that the modification process changed the original structure of lignocellulose components.

XPS analysis

CSP, LCSP, and GCSP were characterized through XPS to determine the changes in surface chemical composition after modification. The surface element composition (atomic fraction, %) results from the XPS wide scan spectra were the same as the above elemental analysis results, further confirming the effectiveness of the graft modification (Fig. 3a).

As shown in Fig. 3b, the four characteristic peaks at 284.8, 286.3, 287.8, and 289.0 eV were attributed to C-C/C-H, C-O, C = N, and C = O, respectively. The relative contents of C functional groups were calculated and are shown in Table 2. The significant

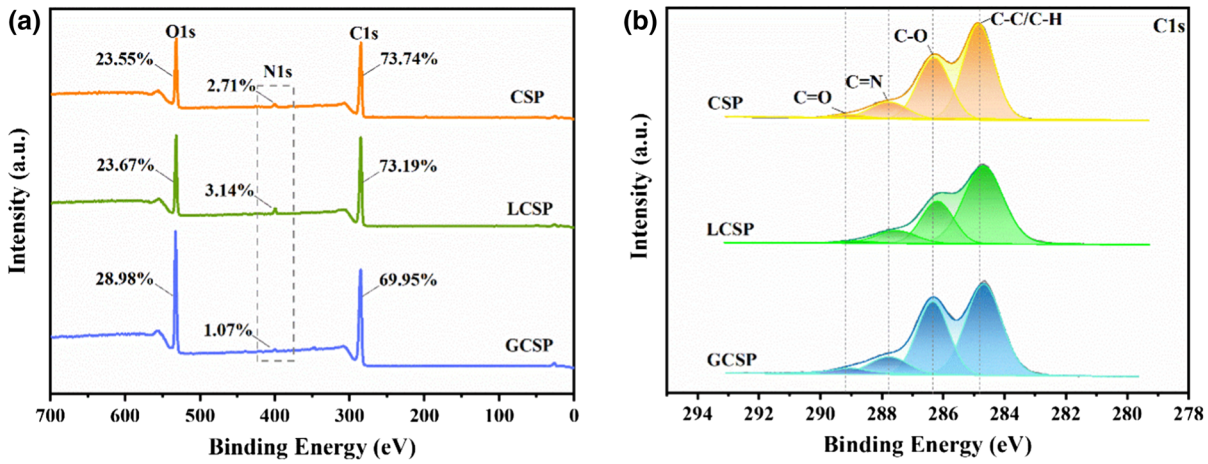

Fig. 3 XPS spectra of CSP, LCSP and GCSP, **a** wide scan and **b** C1s

Table 2 Identification and quantification of C groups on the surface of samples ([a] Binding energy, [b] Atom fraction)

Sample	C–C/C-H		C-O		C = N		C = O	
	BE[a] (eV)	AF[b] (%)	BE (eV)	AF (%)	BE (eV)	AF (%)	BE (eV)	AF (%)
CSP	284.8	52.29	286.3	34.24	287.8	11.11	289.0	2.36
LCSP	284.7	62.43	286.2	25.99	287.6	9.95	288.8	1.63
GCSP	284.7	50.04	286.3	34.29	287.8	10.31	289.0	5.36

increase in the relative content of C–C/C-H in LCSP (from 50.70% to 62.43%) can be attributed to the successful grafting of long alkyl chains from ODA, and the corresponding decrease in the relative content of C-O was due to the oxidation of C-O in cellulose by TEMPO. The highest content of C = N observed in CSP can be explained by the content of crude protein. After pretreatment and oxidation, the crude protein was washed out, and the C = N in CSP was sheltered by ODA, which consists of alkyl carbons. Thus, the relative content of C-C significantly increased, while the relative content of C = N decreased. The relative content of C = O in GCSP was increased because LAC can catalyze covalent bonding between low-molecular-weight compounds and lignin through nucleophilic addition or free radical coupling reactions to produce water-resistant chemical bonds, thereby increasing the content of carbonyl groups on the fiber surface (Milstein et al. 1994). Thus, the guaiacol-mediated reaction seems to allow the activation of phenolic lignin moieties for the grafting of the hydrophobic compound ODG.

CA measurements

The grafting percentages of ODA and ODG on CSP were 18.7% and 10.2%, respectively. The hydrophobicity and oleophilicity of the materials were confirmed using CA measurements. Surfaces with a water CA below 90° are considered to be hydrophilic, those with a water CA above 90° are considered to be hydrophobic, and those with a water CA below 10° are considered to be superhydrophilic (Yu et al. 2020). As shown in Fig. 4a, the water droplet penetrated raw CSP within 1 s, which indicates that the raw material had very poor hydrophobic properties, mainly caused by the presence of hydrophilic cellulose and hemicellulose. Therefore, it is difficult to apply CSP to oil recovery from water as CSP imbibes water and begins to sink fairly rapidly. The substantial enhancement in the hydrophobic character of the surface of the modified CSP was clearly observed from the increase in the (polar) water CA for LCSP to 144.9° and the increase in that for GCSP to 129.7° (Fig. 4c and d), indicating that LAC-mediated grafting of long-alkyl-

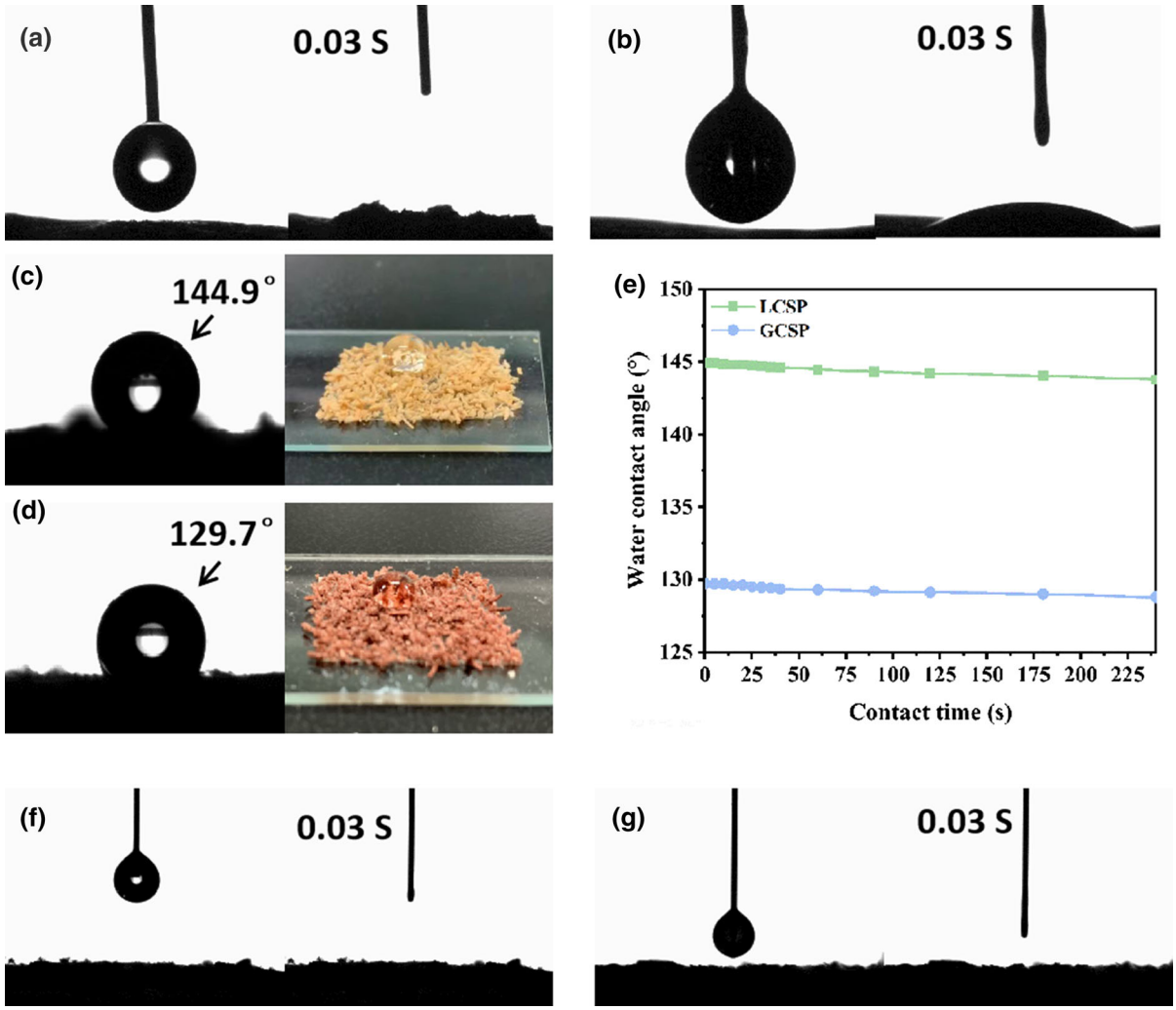

Fig. 4 **a** and **b** Water and oil CAs of CSP. Oil CA (on the right) and pictures of water droplets on the surfaces of LCSP (**c**) and GCSP (**d**). **e** Relationship between contact time and the water CA of LCSP and GCSP. **f** and **g** Diesel CAs of LCSP and GCSP. (All test oils are diesel.)

chain compounds created a low-energy surface and significantly increased hydrophobicity. At a low surface energy, where the affinity between oil molecules and the sorbent surface is much higher than that between water molecules and the sorbent surface, oils are easily sorbed into the sorbent, while water molecules are repelled outside the sorbent assembly due to the high energy barrier (Shin et al. 2020). The relationship between contact time and water CA indicates that the transient hydrophobicity of the material modified by LAC-assisted treatment with TEMPO and guaiacol is good for retaining hydrophobic performance, while that of the material modified by LAC combined with guaiacol-grafted ODG is better, decreasing only by less than 1% after 240 s (Fig. 4e). In addition, the water CAs of both LCSP and GCSP remained above 90° after 24 h. This result indicates that the hydrophobic properties of the materials remained good with the passage of time. Figure 4 (f and g) shows that the oil droplets were absorbed at the moment of contact with the surface of the material, but the oil CA of CSP was always maintained at 16° (Fig. 4b), indicating that the lipophilicity of the modified material was also improved. These results indicated the successful surface modification of CSP from hydrophilic to

hydrophobic and superoleophilic. Thus, LAC-assisted hydrophobization of CSP was performed using guaiacol or TEMPO as the mediator. CSP treated with ODA or ODG showed similar hydrophobic characteristics. These surface characteristics enable LCSP and GCSP to selectively sorb oil and reject water, which allows a smaller mass of sorbent to be used to collect oil and therefore reduces the overall mass of saturated sorbent collected during the treatment of an oil spill.

Stability

Effect of solution pH on the sorption of diesel

Solution pH is an important parameter in the sorption process due to its influence on the surface properties of the sorbent, surface binding sites, and stability of oil particles (Wan Ngah and Hanafiah 2008). The effect of the solution pH on oil–water separation is illustrated in Fig. 5a and b. Low pH impacted the amount of diesel sorbed, especially for GCSP. When the pH increased from 2 to 6, the sorption capacity of LCSP climbed from 11.16 g/g to 12.28 g/g, and the removal rate increased to approximately 98.2%. GCSP also showed the same trend: at low pH values (i.e., pH 2), the sorption capacity was as low as 10.37 g/g. As the pH increased to 8, the sorption capacity reached 12.29 g/g, and the removal rate increased to 98.8%. This variation can be explained by the change in the amounts of protons and hydroxyl ions present in the mixture. Reduced solution pH causes the ionization of previously neutral organic pollutants, thus lowering their favorability to be adsorbed (Ibrahim et al. 2009). In addition, decreased pH mitigates the resistance of oil droplets to coalescence by reducing the emulsion rate (Doshi et al. 2019). The sorption capacity still slightly increased with an additional rise in pH, but this does not mean that high pH is conducive to the sorption of suspended oil. The addition of excessive NaOH to a suspension with residue oil to increase alkalinity could lead to saponification (Ahmad et al. 2003). Diesel undergoes hydrolysis with sodium hydroxide to produce a salt of glycerol and fatty acids, called soap. For this reason, at strong alkaline pH, the residue oil was hydrolyzed and was not extracted by the solvent, thus indirectly yielding a higher percentage of oil sorption (Ahmad et al. 2005a, b). The sorption capacity for diesel oil on LCSP was higher than that on GCSP at pH 1–6, and pH values above 7 were found to give a satisfactory oil uptake of over 98% for both LCSP and GCSP. Hence, pH 7–10 gives an advantage to the treatment process, and no further pH adjustment would be required after this sorption step before the effluent could be discharged.

Effects of ion species and ionic strength on the sorption of diesel

The effects of HPO_4^{2-}, CO_3^{2-}, SO_4^{2-} and Cl^- on the sorption of suspended diesel onto LCSP and GCSP were studied. All ion concentrations were 0.1 mol/L, and all experiments were performed under the same conditions for 1 h. As shown in Fig. 5c, when salt ions were not added to the water, the removal rates of oil by LCSP and GCSP were above 99%. Salt (such as HPO_4^{2-}, CO_3^{2-} and SO_4^{2-}) had a certain influence on the sorption process, especially for LCSP. HPO_4^{2-} and SO_4^{2-} were the salts with the most significant influence on LCSP, and the removal rate was reduced to approximately 90%. However, Cl^- had very little effect on either material. In the presence of different concentrations of Cl^-, the sorption properties of LCSP and GCSP remained stable (Fig. 5d), indicating that the modified materials could maintain a good sorption capacity in seawater.

Sorption kinetics

Kinetic models were used to examine the rate of the sorption process and to propose a potential rate-controlling step, which can be classified into varying adsorption and diffusion processes (Davoodi et al. 2019). The sorption process consists of three steps: (1) film diffusion—i.e., diffusion from the bulk liquid phase through a film surrounding the particle; (2) intraparticle diffusion—i.e., diffusion within the pore fluid of the particle; and (3) mass action—i.e., the reaction of oil molecules with active sites on the surface of the sorbent (Peng et al. 2018). Sorption transfer (diffusion) models are used to describe sorption kinetic results according to the first two steps, while reaction models focus on the last step (Davoodi et al. 2019). To ascertain the sorption mechanism of LCSP and GCSP for the removal of diesel from oily water, the kinetics of sorption were separately modeled by sorption reaction and diffusion models.

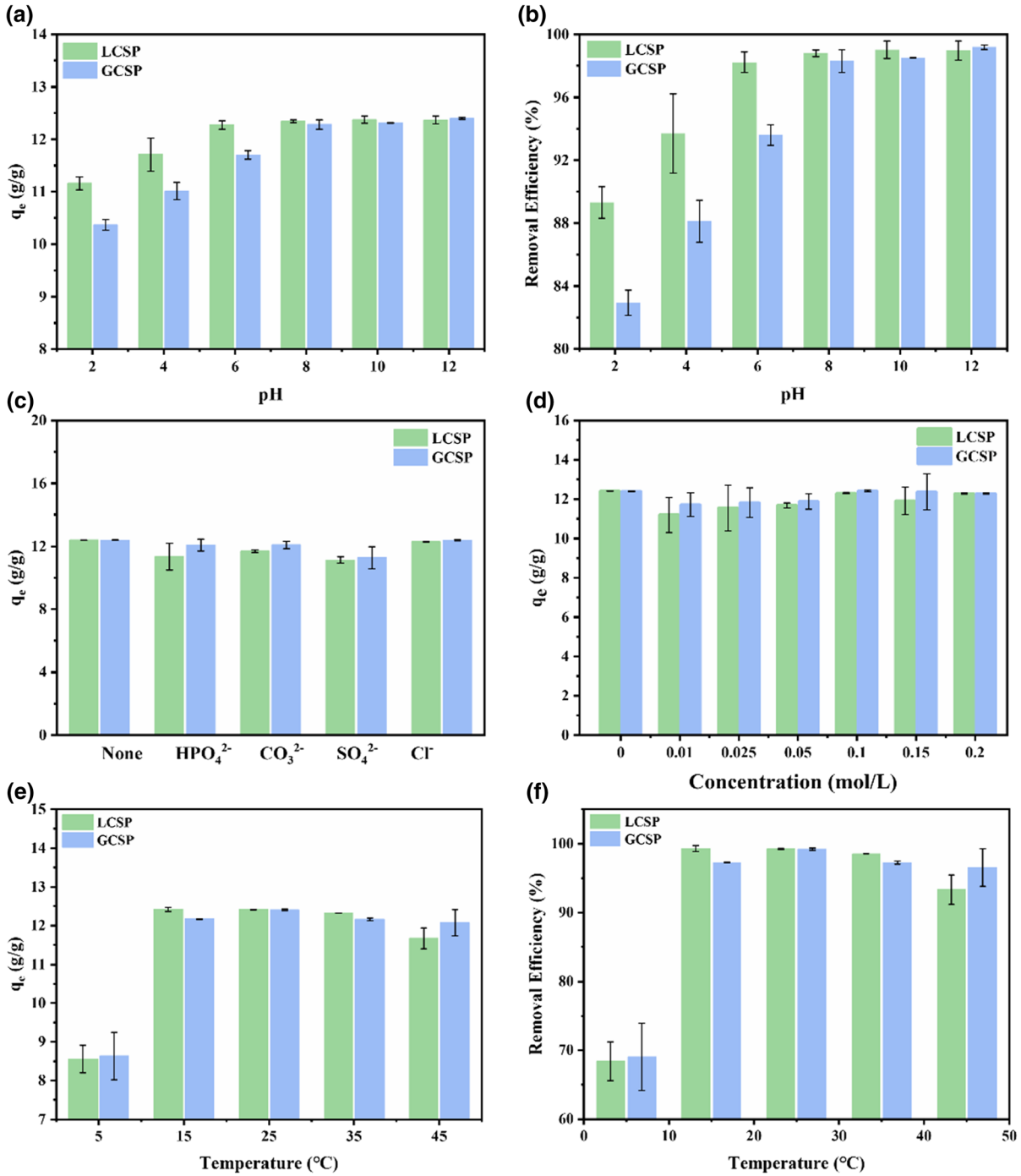

Fig. 5 Effects of pH **a**, **b**, coexisting anions **c** and Cl^- concentration **d**, and temperature **e**, **f**) on diesel absorbency

Sorption reactions are most frequently modeled by pseudo-first-order and pseudo-second-order models (Albadarin et al. 2012). The values of the linear and nonlinear kinetic model parameters are summarized in Table 3. The calculated equilibrium sorption values obtained from nonlinear regression differed from the results obtained from linear regression for the pseudo-first-order kinetic model. The parameters obtained

Table 3 Parameters of kinetic models for suspended diesel adsorption onto modified sorbents

Samples	Kinetic model	Pseudo-first-order model		Pseudo-second-order model	
	Parameters	Linear regression	Nonlinear regression	Linear regression	Nonlinear regression
LCSP	$q_{e,exp}$ (g/g)	12.4102			
	q_e (g/g)	0.0504	12.3993	12.4069	12.4271
	△q (g/g)	12.3598	0.0109	0.0033	0.0278
	k_n (min^{-1})	0.0537	6.8758	10.8273	7.1800
	R^2	0.7436	0.9999	0.9999	0.9998
GCSP	$q_{e,exp}$ (g/g)	12.4190			
	q_e (g/g)	0.2060	12.3484	12.4224	12.3891
	△q (g/g)	12.213	0.0706	0.0034	0.0299
	k_n (min^{-1})	0.0740	0.0145	2.0251	0.0158
	R^2	0.9553	0.9997	0.9999	0.9999

from the slope and intercept of the linear fit are very different from those obtained experimentally. This difference might be because the transformation from a nonlinear to linear pseudo-first-order model implicitly altered the error structure and may have violated the normality assumption of the standard least squares criterion (Raji and Pakizeh 2014). For LCSP, Table 3 shows a good fit with high correlation coefficients for the pseudo-second-order model, and the theoretical q_e values match well with the experimental values. This analysis implies that the sorption process onto the hydrophobic sorbent followed this kinetic model. For GCSP, the regression coefficients of the linearized and nonlinear pseudo-second-order models were higher than those of the pseudo-first-order model. This result indicates that the sorption processes best followed the pseudo-second-order model—i.e., chemical sorption was the rate-controlling step—rather than the pseudo-first-order model. However, chemical sorption is not the only rate-limiting step; other mechanisms may control the rate of sorption, as all mechanisms may be operating simultaneously.

The Boyd model determines whether the main resistance to mass transfer is in the thin film (boundary layer) surrounding the sorbent particle or in the resistance to diffusion inside the pores (Liu et al. 2017). Figure S3a shows the Boyd plot for suspended diesel sorption on LCSP and GCSP. The plots are linear, but they do not pass through the origin, indicating that sorption was governed by film diffusion instead of particle diffusion. To confirm the above observation, ln(1-F) vs. t was plotted, and straight lines deviating from the origin were obtained for all plots, as shown in Figure S3b. These observations further support the fact that the sorption of diesel onto LCSP and GCSP occurred via an internal transport mechanism (Sidik et al. 2012).

The mechanism of diffusion of the sorbed oil from sorption sites on the surface to those available in the interior was analyzed in terms of the intraparticle diffusion model (Gao et al. 2015). The diffusion rates in the first stage (k_1) are larger than those in the second stage (k_2) in Figure S3(c, d). This result can explain why many surface sites were not occupied initially. Therefore, due to the membrane and capillary diffusion mechanism, saturation of the active sites on the outer surface leads directly to rapid adsorption. Over time, the residual amount of oil in the waste liquid becomes very small, and the adsorption rate decreases due to the high oil content adsorbed on the external surface of the adsorbent (Younis et al. 2016). However, according to the low R^2 value of the obtained diffusion model, the diffusion step is not rate limiting. The straight line obtained in the figure does not pass through the origin, which indicates that in addition to intraparticle diffusion, other mass transfer mechanisms occur in the process of removing diesel fuel through LCSP and GCSP (Gupta and Singh 2018). The external mass transport of sorbate and external film diffusion in this sorption system may be very fast. It might be concluded that the large pore size of the

sorbent decreased the contribution of diffusion to oil sorption (Davoodi et al. 2019).

Sorption isotherms

Sorption isotherms are critical for the expression of the surface properties and sorption capacities of sorbents and for understanding the sorption mechanism (Nebaghe et al. 2016). In this study, to optimize the sorption mechanism pathways of LCSP and GCSP, four well-known isotherm models were used to evaluate the experimental data: the Langmuir, Freundlich, Temkin and Dubinin-Radushkevich (D-R) isotherms. All isotherm parameters were calculated from the slopes and intercepts of the fitted straight lines in Table S1 and are summarized in Table 4. The Langmuir isotherm model was derived based on the assumption of monolayer sorption on a structurally homogeneous surface where there were no interactions between molecules sorbed on neighboring sites (Narayanan et al. 2017). The Freundlich model is suitable for describing sorption processes on heterogeneous surfaces of materials, which belong to multilayer sorption (Wang et al. 2016). The Temkin isotherm explicitly considers the interaction between sorbents and sorbates and assumes that the sorption heat decreases linearly and that the process is characterized by a uniform distribution of binding energy (Zheng et al. 2019). The D–R isotherm considers more common characteristics of sorption and is a semiempirical equation (Wang et al. 2012).

The coefficient of determination (R^2) is traditionally employed as credible evidence of the fit of an isotherm model. The R^2 values varied from 0.8356 to 0.9999. From the linear regression coefficients of the four models for the suspended oil sorption processes of the two modified materials, the order of fit to the experimental data was as follows: Langmuir II > Freundlich > Temkin > D-R. The highest R^2 values were obtained for the Type II Langmuir equation. The R_L values of LCSP and GCSP calculated from the initial concentrations of diesel were 0.9986 and 0.9981, respectively. Since the values of R_L were within the range of 0–1, the sorption of diesel onto LCSP and GCSP appeared to be a favorable process. In addition, the small differences in R_L values indicated that the interaction of diesel with LCSP and GCSP might be similar. However, the predicted constant (q_m) obtained from the Langmuir isotherm had a large error with respect to the actual equilibrium data (q_e) for both LCSP and GCSP. These results indicated that it is not appropriate to select the R^2 value in linear regression analysis as the only criterion for identifying the best-fitting model (Ho 2004). Many recent reports have also described this situation. Based on this phenomenon, to evaluate the applicability of the studied models in fitting the equation, empirically, several mathematical error functions were used (Table S1), including the sum of the absolute errors (SAE), the sum of squares (SSE), the root mean square error (RMSE), chi-square ($\chi 2$), the average relative error (ARE), the hybrid fractional error function (HYBRID) and a derivative of Marquardt's percent standard deviation (MPSD) (Ibrahim et al. 2009; Narayanan et al. 2017; Zheng et al. 2019).

The R^2 values of the Freundlich model for LCSP and GCSP were 0.9996 and 0.9997, respectively, slightly lower than those of the Langmuir model (Table 4). However, error analysis indicated that the Freundlich isotherm model presented the lowest error values, showing that the Freundlich model is superior to the Langmuir model. The results indicate that diesel sorption onto LCSP and GCSP followed the heterogeneous multilayer adsorption model. The reason can be illustrated by the complex composition and molecular size of diesel oil (Huang and Yan 2018). In addition, the values of n for LCSP and GCSP were between 1 and 10, establishing a favorable sorption trend onto the material surface. LCSP and GCSP gave the same K_F value (indicating the sorption capacity), echoing the similar results in the experimental data.

The sorbent–sorbate interaction on sorption surfaces and the heat of sorption were investigated by the Temkin isotherm model. As shown in Table 4, the b_T values for the sorption of diesel oil onto LCSP and GCSP were 366.67 kJ mol^{-1} and 362.74 kJ mol^{-1}, respectively, much higher than 80 kJ mol^{-1}, which indicated the chemical nature of sorption, thereby confirming the strong diesel-LCSP and diesel-GCSP interactions. The strong interaction between diesel oil and LCSP or GCSP can be attributed to the similarity in composition between the oil and the grafted long alkyl chains in the adsorption process, leading to the considerable enhancement of the oil-wet performance of the modified material. Furthermore, the b_T value was positive, suggesting that the sorption process was exothermic (Miraboutalebi et al. 2017). Based on the

Table 4 Isotherm parameters and statistical error metrics of LCSP and GCSP

	LCSP				GCSP			
Linear isotherm	Langmuir	Freundlich	Temkin	D-R	Langmuir	Freundlich	Temkin	D-R
Parameters	q_m = 909.09	K_F = 2.5373	B = 766.84	q_{DR} = 13.817	q_m = 666.67	K_F = 2.5373	B = 765.26	q_{DR} = 13.907
	b = 0.0028	n = 1.0151	b_T = 366.67	β = 4E(-07)	b = 0.0038	n = 1.0151	b_T = 362.74	β = 4E(-07)
	R_L = 0.9986			E_{DR} = 1186.8	R_L = 0.9981			E_{DR} = 1183.5
R^2	0.9998	0.9996	0.8910	0.8408	0.9999	0.9997	0.8974	0.8356
SAE	1.8106	1.6946	14.368	27.903	1.4142	1.6564	14.305	28.801
SSE	− 0.9919	− 0.2041	2.8558	8.9287	0.4046	− 0.2047	− 2.9086	9.2512
RMSE	0.3507	0.0722	1.0794	3.1568	0.1431	0.0724	1.0994	3.2708
χ^2	0.0429	0.0332	2.8224	11.628	0.0379	0.0355	2.7498	11.633
ARE	0.4765	0.3691	35.280	129.20	0.2785	0.3949	34.372	129.25
HYBRID	0.6261	0.4746	55.806	161.01	0.3560	0.5142	57.126	166.99
MPSD	2.0065	1.9456	26.512	49.271	1.6863	1.8573	27.810	51.186

different error functions, the D-R model could not offer a reasonably good fit to these experimental data.

Thermodynamic analysis

Temperature is the key parameter used to evaluate sorption performance. The effect of temperature was observed by carrying out sorption experiments at 5, 15, 25, 35, and 45 °C. The oil sorption amounts of LCSP and GCSP were only 9.80 g/g and 9.52 g/g, respectively, at 5 °C. When the temperature was 15 °C, the oil sorption by LCSP increased to 12.42 g/g, and when the temperature was raised to 25 °C, the oil sorption by GCSP also reached 12.41 g/g. Low concentrations of oil were present in very small amounts in solution, and most of the oil was present as suspended oil particles. Particles in this size range in liquids are in Brownian motion and move slowly at low temperatures, reducing the chance of oil particles coming into contact with the surface of the material, which is the reason for the low adsorption capacity at low temperature. As shown in Fig. 5e and f, continuing to increase the temperature resulted in the maximum sorption capacity decreasing to 11.67 g/g and 12.07 g/g at 45 °C, which indicates that the sorption process of suspended diesel onto modified material is exothermic, which is the same as the result obtained from the Temkin isotherm.

Thermodynamic research helps further explain the driving forces and reaction degrees of sorption processes. Table 5 lists the values of the thermodynamic parameters $\triangle G^0$, $\triangle H^0$, and $\triangle S^0$. A negative value of $\triangle G^0$ indicates the spontaneity of the sorption process under study (Gupta and Gupta 2015). As the temperature increased, $\triangle G^0$ decreased, indicating that sorption by the materials at a relatively low temperature was favorable. An exothermic sorption process was represented by a negative value $\triangle H^0$ (enthalpy change). In particular, the exothermic properties of LCSP in the sorption of suspended oil were more obvious than those of GCSP. The positive values of $\triangle S^0$ (entropy change) represented increases in the randomness of the interface (solid/liquid) in the sorption process of suspended oil, indicating that the modified materials had a good affinity for suspended oil (Elanchezhiyan et al. 2016).

Effect of diesel layer thickness on sorption

Figure 6 shows the layer thickness-dependent diesel oil sorption plots for the modified CSP samples. When the oil layer thickness was 6 mm, LCSP and GCSP showed similar sorption capacities. However, with increasing oil layer thickness, the sorption capacity of GCSP became significantly higher than that of LCSP. This result proved that GCSP was superior to LCSP in the sorption of high-concentration oil slicks. As the thickness of the oil layer on the water surface increased, the chance of contact between the sorbent and oil molecules increased, and the chance to directly contact water decreased, so the amount of sorbed oil

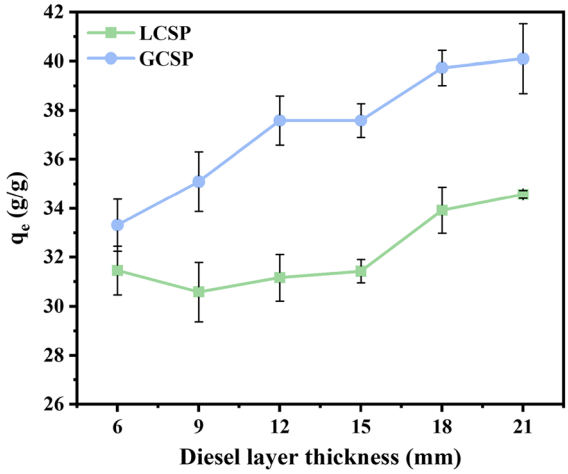

Fig. 6 Effects of diesel layer thickness on sorption

Table 5 Thermodynamic parameters for the adsorption of suspended oil on LCSP and GCSP

Sample	$\triangle G^0$ (KJ/mol)				$\triangle H^0$	$\triangle S^0$
	15°C	25°C	35°C	45°C		
LCSP	− 2239.26	− 2315.54	− 2373.86	− 2304.43	− 1481.14	2.73
GCSP	− 8314.82	− 8667.01	− 8889.67	− 9152.40	− 426.88	27.48

Table 6 Comparison of adsorption properties with those of other biomass-based materials

Material	Method	Oil type	Sorption capacity/ Removal	Water absorption/ CA	Reference
Rice husk ash	Pyrolysis	Diesel	5.02 g/g		Vlaev et al. (2011)
Luffa	Heat treatment	Diesel	> 85%	< 5 g/g	Abdelwahab (2014)
Corn silk	Acetylation	Crude oil	16.68 g/g		Asadpour et al. (2015)
Populus fiber	Acetylation	Corn oil	18.35 g/g	< 152.5°	Yang et al. (2017)
Lignocellulose	Condensation reaction	Machine oil	> 98%	129°	(Kang et al. (2020)
CS fibers	Covalent deposition of ZnO and hydrophobic modification	Crude oil	20.4 g/g	152°	Zang et al. (2016)
Wheat straw	Esterification	Diesel	24.31 g/g		Tang et al. (2018)
Nanocellulose aerogels	Coating with titanium dioxide	Paraffin oil/mineral oil	20–40 wt/ wt	> 90°	Korhonen et al. (2011)
SiO_2–TiO_2 porous nanofibrous membranes	Amino-silanization reaction	Oil/water emulsion	99.26%	149.0°	Wang et al. (2019)
CSP	TEMPO-LAC-octadecylamine system	Suspended diesel	> 99.0%	144.9°	In this study
		Diesel	34.58		
	Guaiacol-LAC-octadecyl gallate system	Suspended diesel	> 98.2%	129.7°	
		Diesel	40.11		

increased. Therefore, better cleaning performance can be obtained. However, for the sorption of oil at lower concentrations, hydrophobic properties are crucial. This point explains why LCSP has higher hydrophobic performance but slightly less surface oil layer sorption than GCSP.

Comparison of sorbents

Table 6 compares various biobased materials prepared with different modification schemes. In addition to inexpensive and easily biodegradable plant biomass materials such as rice husk ash, loofah (agricultural waste), *Populus euphratica* fiber, and wheat straw, biomass parts (corn silk) are used as sorbents to form nanofiber gels. Previously reported capacities are compared to those of our two sorbents using uptake from diesel oil in water. LCSP and GCSP exhibited low pH dependence, promising hydrophobicity, and reasonable oil values. Compared to biomass modified by other processes, biomass modified by pyrolysis has a large energy consumption and low sorption performance. Acetylation and condensation grafting between functional groups (such as cross-linking of diisocyanate) are commonly used modification methods but often require a catalyst, which means the use of harmful chemical reagents. Chemical precipitation or coating of hydrophobic substances can also be used to increase the water CA of the raw materials, but the steps are complicated. In this study, LMS-biocatalyzed grafting of long alkyl chains onto CSP was used to confer the material selective and efficient oil sorption performance, and the modification process was green and easy to operate.

Conclusions

Compared to the sorbent preparation from chemical or physical methods, LMS requires limited chemical pretreatment or activation and avoids the use of hazardous reagents. In addition, LCSP and GCSP prepared by modifying CSP with environmentally friendly LAC (with guaiacol or TEMPO as a mediator) show highly selective oil sorption. A characterization revealed that the modification of CSP by LMS effectively enhanced its surface hydrophobicity and provided oil contact sites to improve the sorption

capacity. The low uptake dependence on temperature, pH, and salinity indicates that fresh water, sea water or process wastewater can be applied. The sorption of suspended diesel by LCSP and GCSP exhibits pseudo-second-order kinetics, and the sorption mechanism is governed by chemisorption. All experimental data fit well with the Freundlich model compared to Langmuir, Temkin and D-R models. The sorption process exhibits an exothermic nature. Moreover, LCSP and GCSP have similar sorption capacities for low-concentration suspended diesel, but GCSP has a stronger sorption capacity for high-concentration floating oil. These factors should allow LMS-modified biobased materials to be used for future oil spill cleanup.

Acknowledgments This work was supported by the National Natural Science Foundation of China (No. 42007323), the Natural Science Foundation of Guangdong province (No. 2018A030313363), the Shenzhen Science & Technology Project (SZIITWDZC2021A01), the Open Fund of Guangdong Provincial Key Laboratory of Petrochemical Pollution Process and Control (No. 2018B030322017), the High-level Professionals and Innovative Teams (No. SZIIT2019KJ024; No. SZIIT2019KJ007), the Guangzhou Municipal Science & Technology Project (201803030001), and the Key-Area Research and Development Program of Guangdong Province (2019B110207001).

Author Contributions DP and LZ conceived and designed the experiments. DP wrote the paper. WL and DP performed the experiments, measurements and characterizations.

Declarations

Conflict of interest The authors declare that they have no conflicts of interest.

Ethical approval This article does not contain any studies with human participants or animals performed by any of the authors. In this experiment, we did not collect any samples of human and animals.

Informed consent Informed consent was obtained from all individual participants included in the study.

References

Abdelwahab O (2014) Assessment of raw luffa as a natural hollow oleophilic fibrous sorbent for oil spill cleanup. Alex Eng J 53(1):213–218

Ahmad AL, Ismail S, Ibrahim N, Bhatia S (2003) Removal of suspended solids and residual oil from palm oil mill effluent. J Chem Technol Biotechnol 78(9):971–978

Ahmad AL, Bhatia S, Ibrahim N, Sumathi S (2005a) Adsorption of residual oil from palm oil mill effluent using rubber powder. Braz J Chem Eng 22(03):371–379

Ahmad AL, Sumathi S, Hameed BH (2005b) Adsorption of residue oil from palm oil mill effluent using powder and flake chitosan: equilibrium and kinetic studies. Water Res 39(12):2483–2494

Albadarin AB, Mangwandi C, Al-Muhtaseb AH, Walker GM, Allen SJ, Ahmad MNM (2012) Kinetic and thermodynamics of chromium ions adsorption onto low-cost dolomite adsorbent. Chem Eng J 179(193):202

Aracri E, Vidal T, Ragauskas AJ (2011) Wet strength development in sisal cellulose fibers by effect of a laccase–TEMPO treatment. Carbohyd Polym 84(4):1384–1390

Asadpour R, Sapari NB, Isa MH, Kakooei S, Orji KU (2015) Acetylation of corn silk and its application for oil sorption. Fibers Polym 16(9):1830–1835

Chen M, Zhao J, Xia L (2008) Enzymatic hydrolysis of maize straw polysaccharides for the production of reducing sugars. Carbohyd Polym 71(3):411–415

Chen C, Zhu X, Chen B (2019) Durable superhydrophobic/superoleophilic graphene-based foam for high-efficiency oil spill cleanups and recovery. Environ Sci Technol 53(3):1509–1517

Davoodi SM, Taheran M, Brar SK, Galvez-Cloutier R, Martel R (2019) Hydrophobic dolomite sorbent for oil spill clean-ups: kinetic modeling and isotherm study. Fuel 251:57–72

Demirel Bayık G, Altın A (2018) Conversion of an industrial waste to an oil sorbent by coupling with functional silanes. J Clean Prod 196:1052–1064

Doshi B, Sillanpaa M, Kalliola S (2018) A review of bio-based materials for oil spill treatment. Water Res 135:262–277

Doshi B, Hietala S, Sirviö JA, Repo E, Sillanpää M (2019) A powdered orange peel combined carboxymethyl chitosan and its acylated derivative for the emulsification of marine diesel and 2T-oil with different qualities of water. J Mol Liq 291:111327

Elanchezhiyan SS, Sivasurian N, Meenakshi S (2016) Enhancement of oil recovery using zirconium-chitosan hybrid composite by adsorptive method. Carbohydr Polym 145:103–113

Filgueira D, Holmen S, Melbø JK, Moldes D, Echtermeyer AT, Chinga-Carrasco G (2017) Enzymatic-assisted modification of thermomechanical pulp fibers to improve the interfacial adhesion with poly(lactic acid) for 3D printing. ACS Sustain Chem Eng 5(10):9338–9346

Fillat U, Roncero MB (2010) Optimization of laccase-mediator system in producing biobleached flax pulp. Biores Technol 101(1):181–187

Gao H, Lv S, Dou J, Kong M, Dai D, Si C, Liu G (2015) The efficient adsorption removal of Cr(vi) by using Fe_3O_4 nanoparticles hybridized with carbonaceous materials. RSC Adv 5(74):60033–60040

Garcia-Ubasart J, Colom JF, Vila C, Gomez Hernandez N, Blanca Roncero M, Vidal T (2012) A new procedure for the hydrophobization of cellulose fibre using laccase and a hydrophobic phenolic compound. Biores Technol 112:341–344

Ge H, Wang C, Liu S, Huang Z (2016) Synthesis of citric acid functionalized magnetic graphene oxide coated corn straw for methylene blue adsorption. Biores Technol 221:419–429

Guo H, Zhang S, Kou Z, Zhai S, Ma W, Yang Y (2015) Removal of cadmium(II) from aqueous solutions by chemically modified maize straw. Carbohyd Polym 115:177–185

Gupta H, Gupta B (2015) Adsorption of polycyclic aromatic hydrocarbons on banana peel activated carbon. Desalin Water Treat 57(20):9498–9509

Gupta H, Singh S (2018) Kinetics and thermodynamics of phenanthrene adsorption from water on orange rind activated carbon. Environ Technol Innov 10:208–214

Ho Y-S (2004) Selection of optimum sorption isotherm. Carbon 42(10):2115–2116

Hokkanen S, Bhatnagar A, Sillanpaa M (2016) A review on modification methods to cellulose-based adsorbents to improve adsorption capacity. Water Res 91:156–173

Huang J, Yan Z (2018) Adsorption mechanism of oil by resilient graphene aerogels from oil-water emulsion. Langmuir 34(5):1890–1898

Ibrahim S, Ang HM, Wang S (2009) Removal of emulsified food and mineral oils from wastewater using surfactant modified barley straw. Biores Technol 100(23):5744–5749

Ibrahim S, Wang S, Ang HM (2010) Removal of emulsified oil from oily wastewater using agricultural waste barley straw. Biochem Eng J 49(1):78–83

Indran S, Raj RE, Sreenivasan VS (2014) Characterization of new natural cellulosic fiber from cissus quadrangularis root. Carbohyd Polym 110:423–429

Jiang T, Liang Y-D, He Y-J, Wang Q (2015) Activated carbon/$NiFe_2O_4$ magnetic composite: a magnetic adsorbent for the adsorption of methyl orange. J Environ Chem Eng 3(3):1740–1751

Kacurakova M, Belton PS, Wilson RH, Hirsch J, Ebringerova A (1998) Hydration properties of xylan-type structures: an FTIR study of xylooligosaccharides. J Sci Food Agric 77:38–44

Kang L, Wang B, Zeng J, Cheng Z, Li J, Xu J, Gao W, Chen K (2020) Degradable dual superlyophobic lignocellulosic fibers for high-efficiency oil/water separation. Green Chem 22(2):504–512

Korhonen JT, Kettunen M, Ras RH, Ikkala O (2011) Hydrophobic nanocellulose aerogels as floating, sustainable, reusable, and recyclable oil absorbents. Acs Appl Mater Inter 3(6):1813–1816

Kudanga T, Prasetyo EN, Sipila J, Guebitz GM, Nyanhongo GS (2010) Reactivity of long chain alkylamines to lignin moieties: implications on hydrophobicity of lignocellulose materials. J Biotechnol 149(1–2):81–87

Kudanga T, Nyanhongo GS, Guebitz GM, Burton S (2011) Potential applications of laccase-mediated coupling and grafting reactions: a review. Enzyme Microb Technol 48(3):195–208

Lamichhane S, Bal Krishna KC, Sarukkalige R (2016) Polycyclic aromatic hydrocarbons (PAHs) removal by sorption: a review. Chemosphere 148:336–353

Lavoine N, Desloges I, Dufresne A, Bras J (2012) Microfibrillated cellulose – Its barrier properties and applications in cellulosic materials: a review. Carbohyd Polym 90(2):735–764

Li D, Zhu FZ, Li JY, Na P, Wang N (2013) Preparation and characterization of cellulose fibers from corn straw as natural oil sorbents. Ind Eng Chem Res 52(1):516–524

Li R, Ren J, Xu Y, Zhang G, Wang D, Wu Z, Cai D (2019) Hydrophobic nano sponge for efficient removal of diesel fuel from water and soil. Sci Total Environ 688:1124–1136

Liu P, Wang Q, Zheng C, He C (2017) Sorption of sulfadiazine, norfloxacin metronidazole, and tetracycline by granular activated carbon: kinetics, mechanisms, and isotherms. Water Air Soil Pollut 228(4):1–4

Milstein O, Hiittermann A, Friind R, Liidemann H-D (1994) Enzymatic co-polymerization of lignin with low-molecular mass compounds. Appl Microbiol Biotechnol 40:760–767

Miraboutalebi SM, Nikouzad SK, Peydayesh M, Allahgholi N, Vafajoo L, McKay G (2017) Methylene blue adsorption via maize silk powder: Kinetic, equilibrium, thermodynamic studies and residual error analysis. Process Saf Environ Prot 106:191–202

Moldes D, Vidal T (2011) New possibilities of kraft pulp biobleaching with laccase and sulfonated mediators. Process Biochem 46(3):656–660

Moosai R, Dawe RA (2003) Gas attachment of oil droplets for gas flotation for oily wastewater cleanup. Sep Purif Technol 33(3):303–314

Narayanan N, Gupta S, Gajbhiye VT, Manjaiah KM (2017) Optimization of isotherm models for pesticide sorption on biopolymer-nanoclay composite by error analysis. Chemosphere 173:502–511

Navarathna CM, Bombuwala Dewage N, Keeton C, Pennisson J, Henderson R, Lashley B, Zhang X, Hassan EB, Perez F, Mohan D, Pittman CU Jr, Mlsna T (2020) Biochar adsorbents with enhanced hydrophobicity for oil spill removal. ACS Appl Mater Interfaces 12(8):9248–9260

Nebaghe KC, El Boundati Y, Ziat K, Naji A, Rghioui L, Saidi M (2016) Comparison of linear and non-linear method for determination of optimum equilibrium isotherm for adsorption of copper(II) onto treated martil sand. Fluid Phase Equilib 430:188–194

Oliveira LMTM, Oliveira LFAM, Sonsin AF, Duarte JLS, Soletti JI, Fonseca EJS, Ribeiro LMO, Meili L (2020) Ultrafast diesel oil spill removal by fibers from silk-cotton tree: Characterization and sorption potential evaluation. J Clean Prod 263:121448

Peng D, Lan Z, Guo C, Yang C, Dang Z (2013) Application of cellulase for the modification of corn stalk: leading to oil sorption. Biores Technol 137:414–418

Peng D, Ouyang F, Liang X, Guo X, Dang Z, Zheng L (2018) Sorption of crude oil by enzyme-modified corn stalk vs. chemically treated corn stalk. J Mol Liq 255:324–332

Prendergast DP, Gschwend PM (2014) Assessing the performance and cost of oil spill remediation technologies. J Clean Prod 78:233–242

Raji F, Pakizeh M (2014) Kinetic and thermodynamic studies of Hg(II) adsorption onto MCM-41 modified by ZnCl2. Appl Surf Sci 301:568–575

Schneider WDH, Bolaño Losada C, Moldes D, Fontana RC, de Siqueira FG, Prieto A, Martínez MJ, Martínez ÁT, Dillon AJP, Camassola M (2019) A sustainable approach of enzymatic grafting on eucalyptus globulus wood by laccase from the newly isolated white-rot basidiomycete

marasmiellus palmivorus VE111. ACS Sustainable Chemistry & Engineering 7(15):13418–13424
Shin Y, Han KS, Arey BW, Bonheyo GT (2020) Cotton fiber-based sorbents for treating crude oil spills. ACS Omega 5(23):13894–13901
Sidik SM, Jalil AA, Triwahyono S, Adam SH, Satar MAH, Hameed BH (2012) Modified oil palm leaves adsorbent with enhanced hydrophobicity for crude oil removal. Chem Eng J 203:9–18
Sidiras D, Batzias F, Konstantinou I, Tsapatsis M (2014) Simulation of autohydrolysis effect on adsorptivity of wheat straw in the case of oil spill cleaning. Chem Eng Res Des 92(9):1781–1791
Singh G, Arya SK (2019) Utility of laccase in pulp and paper industry: a progressive step towards the green technology. Int J Biol Macromol 134:1070–1084
Skals PB, Krabek A, Nielsen PH, Wenzel H (2007) Environmental assessment of enzyme assisted processing in pulp and paper industry. Int J Life Cycle Assess 13(2):124–132
Tang M, Zhang R, Pu Y (2018) Wheat straw modified with palmitic acid as an efficient oil spill adsorbent. Fibers Polym 19(5):949–955
Thilagavathi G, Praba Karan C, Das D (2018) Oil sorption and retention capacities of thermally-bonded hybrid nonwovens prepared from cotton, kapok, milkweed and polypropylene fibers. J Environ Manage 219:340–349
Tran VS, Ngo HH, Guo W, Zhang J, Liang S, Ton-That C, Zhang X (2015) Typical low cost biosorbents for adsorptive removal of specific organic pollutants from water. Biores Technol 182:353–363
Vafakhah S, Bahrololoom ME, Bazarganlari R, Saeedikhani M (2014) Removal of copper ions from electroplating effluent solutions with native corn cob and corn stalk and chemically modified corn stalk. J Environ Chem Eng 2(1):356–361
Vlaev L, Petkov P, Dimitrov A, Genieva S (2011) Cleanup of water polluted with crude oil or diesel fuel using rice husks ash. J Taiwan Inst Chem Eng 42(6):957–964
Wan Ngah WS, Hanafiah MAKM (2008) Adsorption of copper on rubber (Hevea brasiliensis) leaf powder: Kinetic, equilibrium and thermodynamic studies. Biochem Eng J 39(3):521–530
Wang H, Ma L, Cao K, Geng J, Liu J, Song Q, Yang X, Li S (2012) Selective solid-phase extraction of uranium by salicylideneimine-functionalized hydrothermal carbon. J Hazard Mater 229–230:321–330
Wang H, Xu X, Ren Z, Gao B (2016) Removal of phosphate and chromium(vi) from liquids by an amine-crosslinked nano-Fe_3O_4 biosorbent derived from corn straw. RSC Adv 6(53):47237–47248
Wang Y, Wang B, Wang Q, Di J, Miao S, Yu J (2019) Amino-functionalized porous nanofibrous membranes for simultaneous removal of oil and heavy-metal ions from wastewater. ACS Appl Mater Interfaces 11(1):1672–1679
Wu MN, Maity JP, Bundschuh J, Li CF, Lee CR, Hsu CM, Lee WC, Huang CH, Chen CY (2017) Green technological approach to synthesis hydrophobic stable crystalline calcite particles with one-pot synthesis for oil-water separation during oil spill cleanup. Water Res 123:332–344
Yang SZ, Jin HJ, Wei Z, He RX, Ji YJ, Li, XM, Yu, S.P. (2009) Bioremediation of oil spills in cold environments: a review. Pedosphere 19(3):371–381
Yang S, He W-T, Fu Y, Zhang Y, Yuan T-Q, Sun R-C (2017) A bio-based coating onto the surface populus fiber for oil spillage cleanup applications. Ind Crops Prod 98:38–45
Yang W-J, Yuen ACY, Li A, Lin B, Chen TBY, Yang W, Lu H-D, Yeoh GH (2019) Recent progress in bio-based aerogel absorbents for oil/water separation. Cellulose 26(11):6449–6476
Younis SA, El-Sayed M, Moustafa YM (2016) Modeling and optimization of oil adsorption from wastewater using an amorphous carbon thin film fabricated from wood sawdust waste modified with palmitic acid. Environmental Processes 4(1):147–168
Yu T, Halouane F, Mathias D, Barras A, Wang Z, Lv A, Lu S, Xu W, Meziane D, Tiercelin N, Szunerits S, Boukherroub R (2020) Preparation of magnetic, superhydrophobic/superoleophilic polyurethane sponge: Separation of oil/water mixture and demulsification. Chem Eng J 384:123339
Zang D, Zhang M, Liu F, Wang C (2016) Superhydrophobic/superoleophilic corn straw fibers as effective oil sorbents for the recovery of spilled oil. J Chem Technol Biotechnol 91(9):2449–2456
Zhang K, Chen T (2018) Dried powder of corn stalk as a potential biosorbent for the removal of iodate from aqueous solution. J Environ Radioact 190–191:73–80
Zhang T, Li Z, Lü Y, Liu Y, Yang D, Li Q, Qiu F (2018) Recent progress and future prospects of oil-absorbing materials. Chinese J Chem Eng 27(6):1282–1295
Zhang G, Li Y, Gao A, Zhang Q, Cui J, Zhao S, Zhan X, Yan Y (2019) Bio-inspired underwater superoleophobic PVDF membranes for highly-efficient simultaneous removal of insoluble emulsified oils and soluble anionic dyes. Chem Eng J 369:576–587
Zhang Y, Peng D, Luo Y, Huang D, Guo X, Zhu L (2020) Cellulase modified waste biomass to remove sulfamethazine from aqueous solutions. Sci Total Environ 731:138806
Zheng L, Yang Y, Meng P, Peng D (2019) Absorption of cadmium (II) via sulfur-chelating based cellulose: Characterization, isotherm models and their error analysis. Carbohyd Polym 209:38–50
Zhou Q, Yan B, Xing T, Chen G (2019) Fabrication of superhydrophobic caffeic acid/Fe@cotton fabric and its oil-water separation performance. Carbohyd Polym 203:1–9